NASA TECHNICAL MEMORANDUM

NASA TM X-73455

EXPERIMENTAL INVESTIGATION OF THE EXCESS CHARGE AND TIME CONSTANT OF MINORITY CARRIERS IN THE THIN DIFFUSED LAYER OF 0.1 OHM-CM SILICON SOLAR CELLS

by M. P. Godlewski and Henry W. Brandhorst, Jr.
Lewis Research Center
Cleveland, Ohio 44135

F. A. Lindholm
University of Florida
Gainesville, Florida

and C. T. Sah
University of Illinois
Urbana, Illinois

TECHNICAL PAPER to be presented at
Materials Research Conference sponsored by
the American Institute of Mining, Metallurgical, and Petroleum Engineers
Salt Lake City, Utah, June 23-25, 1976

EXPERIMENTAL INVESTIGATION OF THE EXCESS CHARGE AND TIME CONSTANT OF MINORITY CARRIERS IN THE THIN DIFFUSED LAYER OF 0.1 OHM-CM SILICON SOLAR CELLS

by M. P. Godlewski and Henry W. Brandhorst, Jr.

NASA-Lewis Research Center
Cleveland, Ohio

and F. A. Lindholm

University of Florida
Gainesville, Florida

and C. T. Sah

University of Illinois
Urbana, Illinois

E-2814

INTRODUCTION

The measured open-circuit voltage of 0.1 Ω-cm n on p silicon solar cells is about 100 mv lower than predicted by simple diffusion theory (1). It has been shown (2) that the Air Mass Zero (AMO) conversion efficiency of silicon solar cells can be increased to about 18% providing the processes limiting open-circuit voltage are overcome.

Dark and illuminated electrical measurements strongly suggest that the low open-circuit voltage in 0.1 Ω-cm solar cells is related to an excessively high diode saturation current resulting from processes occuring in the diffused layer. Theoretical analyses have shown that either high recombination rates (3) or bandgap narrowing effects (1) can explain the high saturation current. There is, however, insufficient experimental information about the diffused layer properties to assess the relative importance of these physical processes.

The purpose of this paper is to present an experimental method that can be used to interpret the relative roles of bandgap narrowing and recombination processes in the diffused layer. This method involves measuring the device time constant by open-circuit voltage decay and the base region diffusion length by X-ray excitation. A unique illuminated diode method is used to obtain the diode saturation current. These data are interpreted using a simple model to determine individually the minority carrier lifetime and the excess charge. These parameters are then used to infer the relative importance of bandgap narrowing and recombination processes in the diffused layer.

THEORY

The theoretical work of Lindholm and Sah (3, 4) describes a straightforward charge-control treatment to identify the physical mechanisms controlling carrier transport in the diffused layer (emitter). The solar cell current (I) can be expressed as

$$I = I_D + I_L \tag{1}$$

where I_D and I_L are the dark diode and light generated current, respectively. The diode current can be written as the sum of emitter (I_E), space charge (I_{sc}), and base currents (I_B):

$$I_D = I_E + I_B + I_{sc} \tag{2}$$

In the range of voltages for which the space charge region current is negligible, the diode current (I_D) is the sum of the emitter and base region components:

$$I_D = I_E + I_B \tag{3}$$

From Shockley's diode theory (5), the diode current can also be expressed:

$$I_D = I_o \left(\exp \frac{qV}{kT} - 1\right) \tag{4}$$

where the diode saturation current (I_o) is the sum of the emitter and base region components (I_{EO}, I_{BO}).

By charge-control theory (3, 4), I_D can be written in terms of the stored charge (Q) and time constant τ:

$$I_D = \frac{Q_E}{\tau_E} + \frac{Q_B}{\tau_B} \tag{5}$$

Since, for the voltage range under consideration, $Q = Q_O (\exp \frac{qV}{kT} - 1)$, where Q_O is a reference charge, equation 3 can be written as

$$I_D = \left(\frac{Q_{EO}}{\tau_E} + \frac{Q_{BO}}{\tau_B}\right)\left(\exp \frac{qV}{kT} - 1\right) \tag{6}$$

In this model the diode saturation current is expressed as:

$$I_o = \frac{Q_{EO}}{\tau_E} + \frac{Q_{BO}}{\tau_B} \tag{7}$$

where $Q_{BO} = \frac{qn_i^2 L_B}{N_B}$ for a base of constant doping. Here L_B and N_B are the minority carrier diffusion length and the impurity concentration in the base region. From (4) I_o can be written as:

$$I_o = \frac{Q_{EO} + Q_{BO}}{\tau_o} \tag{8}$$

where τ_o is the dominant normal mode or the reciprocal of the dominant natural frequency of the device as determined by measuring the open-circuit voltage decay.

Equations 7 and 8 involve six parameters Q_{EO}, τ_E, Q_{BO}, τ_B, I_o and τ_o. They form a basis for the separate determination of Q_{EO}, τ_E, whereas previously only the Q_{EO}/τ_E ratio has been evaluated. The reference charge (Q_{EO}) can be associated with bandgap narrowing, while the recombination time (τ_E) reflects recombination effects in the diffused layer. The experimental methods employed to obtain these parameters are described in the next section.

EXPERIMENTAL METHODS

A. Device Fabrication

Six n on p silicon solar cells shown in figure 1 were constructed using a standard processing technique. The 1 x 2 cm, vacuum float zone, < 111 > orientation, 0.1 ohm-cm, p-type silicon wafers were first chemically polished in an HF -HNO_3 - glacial acetic acid solution. The wafers were then phosphorus diffused in a $POCl_3$ atmosphere for 45 minutes at a temperature of 880° C to form the p-n junction. The calculated junction depth is about 0.2 μm. After removal of the phosphorus oxide glass with HF, silver-aluminum contacts were thermally evaporated to form the large area p-side contact and the gridded contact to the thin diffused layer. Contact adherence was insured by sintering the cells in argon at 550° C for several minutes.

B. Electrical Measurements

Current-Voltage

Dark forward and illuminated current-voltage characteristics were measured for each cell using a calculator controlled data acquisition system. A xenon-light solar simulator was used for the AMO (outer space condition) illuminated measurements. The open-circuit voltages (V_{oc}) and short-circuit currents (I_{sc}), of these 0.1 Ω-cm silicon cells are shown in Table I.

Open Circuit Voltage Decay

The time constants characteristic of small area sections of the test cells were measured using the open-circuit voltage decay method (6, 7) and the measurement circuitry shown in Figure 2. The devices were forward

biased with a one millisecond duration square wave voltage pulse. The voltage decay, shown in figure 3, was displayed on a Tektronix 555 oscilloscope with a Type L plug-in unit and photographed. The decay time constants (τ_o) shown in Table I were measured in the 0.55 to 0.63 voltage decay range. The slope factor (A) determined from the illuminated I-V characteristics is found to be nearly unity in this range.

Diode Saturation Current

The illuminated method used to obtain the current-voltage characteristics involves measurement of the V_{oc} and I_{sc} developed by the cell under various levels of light intensity. Advantages of this method, compared to that utilizing the I-V characteristic of a dark diode, include minimization of series resistance effects and duplication of effects of illumination on recombination center states. The method permits the identification of the diffusion dominated ($A \approx 1$) portion of the forward I-V characteristic, and hence an accurate extrapolation of this curve to determine the diffusion-controlled diode saturation current. The saturation currents (I_o) for each cell are shown in Table I. Typical dark forward and illuminated current-voltage characteristics are shown in figure 4.

P-Base Diffusion Length and Recombination Time

The minority carrier base region diffusion lengths (L_B) (and τ_B) determined by the X-ray method (8) are shown in Table I. In this technique the current generated by a uniformly absorbed beam of X-rays and collected across the junction is proportional to the base region minority carrier diffusion length. The base recombination time and the diffusion length are related by the expression, $L^2_B = D_B\tau_B$.

DISCUSSION

The emitter charge (Q_{EO}) and recombination time (τ_e) calculated using the experimental data of Table I and equations 7 and 8 from the charge-control model are given in Table II. Conventional diode theory (3) unmodified by bandgap narrowing effects predicts an emitter charge (Q_{EO}) of about 1×10^{-22} coulombs/cm^2 for the cell structures considered here. The charge deduced by the experimental methods shown here is about 5 orders of magnitude greater than this predicted value. As discussed in (3, 4) the presence of a large stored emitter charge indicates a first order influence of bandgap narrowing.

The emitter recombination times shown in Table II are about 0.2×10^{-6} sec. Using equation 7 and the emitter charge from conventional theory yields a value of the emitter contribution to I_o that is small compared to that from the base region. This suggests that τ_E is sufficiently long such that major improvements in the open-circuit voltage of the cells considered here will be achieved by reductions in the emitter charge rather than improvements in the recombination time.

CONCLUSION

This paper has presented an experimental method for individually determining the emitter stored charge and recombination time. Previous work has only been able to assess the ratio of these device parameters. As a result of the findings presented here, it is concluded that band-gap narrowing effects have a first order significance in determining the charge carrier transport controlling the open-circuit voltage of 0.1 Ω-cm silicon solar cells.

REFERENCES

1. Godlewski, M. P.; Brandhorst, H. W., Jr.; and Baraona, C. R.: Effects of High Doping Levels on Silicon Solar Cell Performance, Eleventh IEEE Photovoltaic Specialists Conference Proceedings, 1975, pg. 32.

2. Brandhorst, Henry W., Jr.: Solar Cell Efficiency - Practice and Promise, Ninth Photovoltaic Specialists Conference Proceedings, May 2-5, 1976.

3. Lindholm, F. A.; Li, S.; Sah, C. T.: Eleventh Photovoltaic Specialists Conference Proceedings, 1975, Pg. 3.

4. Lindholm, Fredrik A.; Sah, C. Tang: Normal Modes of pn Junction Devices for Material Parameter Determination, J Applied Physics, September 1976, in press.

5. Shockley, W.: Bell System Technical J., vol. 28, pp 435-489, July 1949.

6. Lederhandler, S. R.; and Giacoletto, L. J.: Proc. Inst. Radio Engrs. 43, 477 (1955).

7. Bassett, R. J.; Fulop, W.: and Hogarth, C. A.: Bt. J. Electronics, vol. 35, No. 2, 177-192 (1973).

8. Lamneck, J. H., Jr.: Diffusion Lengths in Silicon Obtained by an X-ray Method, NASA TM X-1894, Oct. 1969.

TABLE I

CHARACTERISTICS OF 0.1 Ω-CM
SILICON SOLAR CELLS, RUN 526

CELL #	V_{oc} (VOLTS)	I_{sc} (mA)	L_B (MICRONS)	I_o (AMP X 10^{-12})	τ_o* (μsec)
P-1	.595	39	32	3.9	.16
Q-2	.612	41.2	89	2.2	.24
Q-3	.604	41.2	86	2.9	.18
K-1	.605	41	81	2.8	.18
K-2	.600	40	82	3.4	.17
K-3	.607	42	84	2.5	.16
*MEASURED IN THE 0.55 TO 0.63 VOLTAGE DECAY RANGE					

TABLE II

DIFFUSED LAYER RECOMBINATION TIME
AND CHARGE USING TABLE I DATA AND
EQUATIONS 7 AND 8

CELL	τ_E μsec	Q_{EO} COULOMBS/CM^2 X 10^{-17}
P-1	.16	2.0
Q-2	.23	1.2
Q-3	.18	3.5
K-1	.18	1.4
K-2	.17	1.4
K-3	.16	1.4

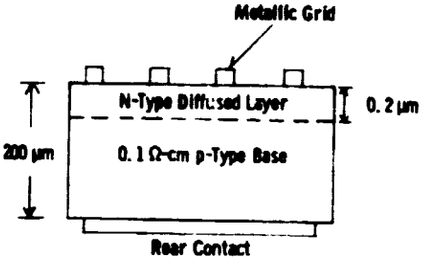

Fig. 1 - Cross Section of 0.1 Ω-cm Silicon Solar Cell

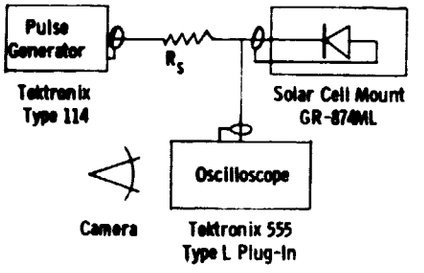

Fig. 2 - Open-Circuit Voltage Decay Apparatus

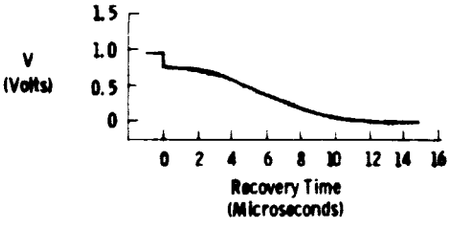

Fig. 3 - Open-Circuit Voltage Decay of 0.1 Ω-cm Cell 526-Q3

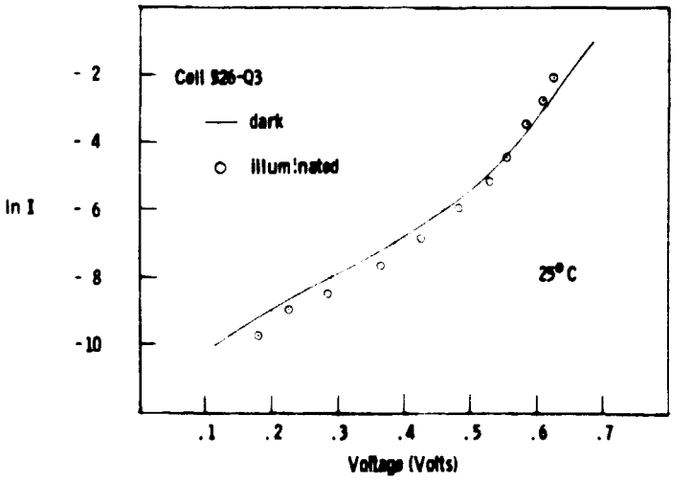

Fig. 4 - Forward Current-Voltage Characteristics of 0.1 Ω-cm Silicon Cell Measured by Dark and Illuminated Bias Methods